Numerical modeling of the effect of energy-separation in the ranque-hilsch tube

Boris L. Ivanov[1]*, *Bulat G.* Ziganshin[1], *Andrey V.* Dmitriev[1], *Maxim A.* Lushnov[1] and *Manuel O.* Binelo[2]

[1]Kazan State Agrarian University, 420015 Kazan, Russia
[2]Regional University of the Northwest of Rio Grande do Sul, Brazil

Abstract. Currently, there are a lot of applications of vortex technologies. The vortex effect is used in gas-dynamic cold generators and vortex cooling chambers. Vortex devices are also used as dehumidifiers, separators, for cooling and heating hydraulic fluids, separating two-phase media, gas mixtures, evacuating, etc. Scientists study the applicability of vortex equipment for traditional and freeze-drying of agricultural products. However, the influence of geometric parameters of vortex devices on the productivity and energy efficiency of temperature separation of gas flows is poorly studied. Research aimed at finding opportunities and expanding the field of application of vortex tubes is an urgent task. The paper describes two-dimensional and three-dimensional mathematical models of the swirling gas flow arising in a vortex tube. It presents results of its implementation in the Ancs-Fluent software package. Thermodynamic and hydrodynamic characteristics confirm the effect of temperature separation in a vortex tube. The dependences of temperature separation on the swirl angle and inlet pressure were obtained. For a two-dimensional vortex tube model, calculations were carried out using various turbulence models. The influence of the cross-sectional area at the hot gas flow outlet on temperature separation was studied.

1 Introduction

In the modern world, the use of the vortex effect for generating heat and cold is becoming more and more relevant [1, 2]. Vortex devices are used as a source of heat and cold for thermal exposure and to improve technical parameters of nebulizers when dispersing various media [3–5].

The effect of temperature separation of the flow or the vortex effect was discovered in 1931 by the French engineer Joseph Ranque during experiments on industrial cyclones. He also developed the design of a vortex tube and received the first patent for the manufacture of a vortex tube. In 1946, the German scientist Robert Hilsch published the results of his experiments on vortex tubes, improving the construction of J. Ranque's tube, and the phenomenon gained fame around the world. R. Hilsch introduced the classical criteria and quantities that are still used in calculations. Vortex tubes are called by the name of their inventors – Ranque's tubes or Ranque-Hilsch's tubes [6, 7].

Vortex tubes have such advantages as simplicity of design, compactness; low production costs, high reliability; significant speed; implementation of several processes simultaneously: phase separation, cooling and heating of the gas flow [8, 9].

Positive qualities of vortex devices make it possible to make engineering systems manufacturable, speedy, easy to manufacture and operate, safe and environmental friendly [10].

There are various types of vortex tube designs [11]. However, despite the relevance of the energy separation effect in various technological processes, there is no general theory of the vortex effect. It is due to the difficulty of studying the complexity of the flow in the vortex tube and significant turbulent pulsations [12, 13]. Therefore, the study of the Ranque-Hilsch effect and numerical simulation of flow energy separation in a vortex tube remain urgent tasks.

2 Materials and Methods

Over many research years, the main types of vortex tubes have been developed and classified: straight-through, counter-current, double-circuit, and single-flow (with one flow) [14].

Consider the principle of energy separation in a countercurrent vortex tube (Figure 1).

Compressed air enters the vortex chamber and, during the screw process, a free vortex is formed in the vortex tube, its temperature increases at the periphery and decreases at the center of the vortex. Heated gas exits through the energy separation chamber, and cooled gas exits through the opposite end [15].

To carry out a numerical study, a classical countercurrent vortex tube design with certain geometric parameters was developed (Figure 2). It consists of vortex chamber 1 (swirl) with a tangential supply of compressed air, opening for the exit of cold gas 2 and

* Corresponding author: littab@mail.ru

opening for the exit of hot gas 3 and energy separation chamber 4, which is a hollow pipe.

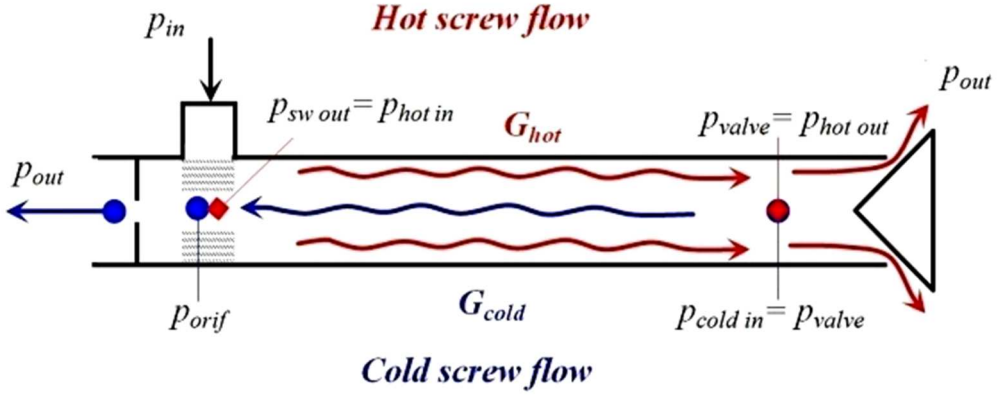

Fig. 1. The technological scheme of energy separation in a vortex tube

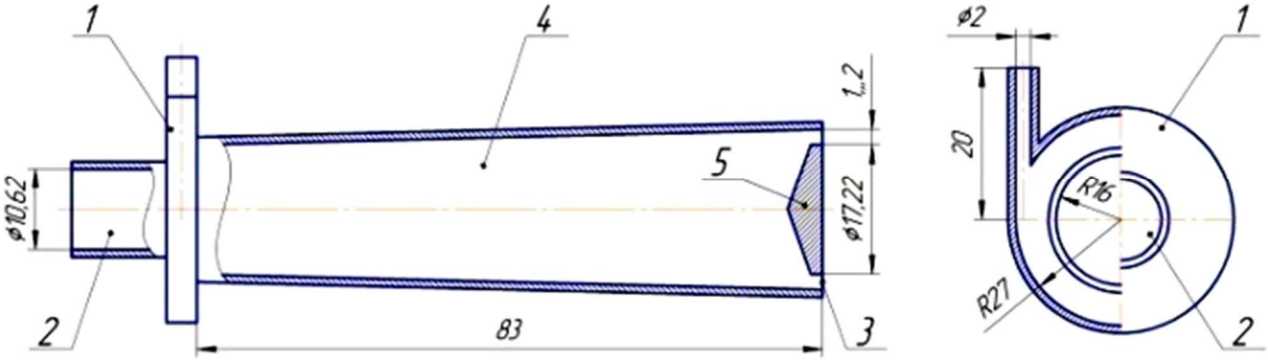

Fig. 2. The geometric region of the vortex tube: 1 – vortex chamber; 2 – hole for the removal of cold gas; 3 – hole for the removal of hot gas; 4 – energy separation chamber; 5 – throttle.

The goal of the research is to study the Ranque-Hilsch effect and simulate temperature separation of the flow in a vortex tube based on the Ansys-Fluent software package.

Numerical modeling of the energy separation effect in a vortex tube was carried out in two-dimensional and three-dimensional approximations.

When modeling the energy separation process in a vortex tube, the following assumptions were adopted [16, 17]:

1) The gas flow model in the vortex tube is stationary, turbulent and swirling;

2) Compressible viscous ideal gas is considered as a medium.

For the mathematical description of the nature of the two-dimensional gas flow, the following equations were used:

1) The continuity equation:

$$\frac{\partial \rho u}{\partial x} + \frac{1}{r}\frac{\partial \rho v r}{\partial r} = 0.$$

2) The equation for a longitudinal change in momentum:

$$\frac{\partial \rho u^2}{\partial x} + \frac{1}{r}\frac{\partial \rho u v r}{\partial r} = -\frac{\partial \rho}{\partial x} + \frac{\partial}{\partial x}\left[(\mu + \mu_t)\left(2\frac{\partial u}{\partial x} - \frac{2}{3}\left(\frac{\partial u}{\partial x} + \frac{1}{r}\frac{\partial v r}{\partial r}\right)\right)\right] +$$
$$+ \frac{1}{r}\frac{\partial}{\partial r}\left[(\mu + \mu_t) r\left(\frac{\partial u}{\partial r} + \frac{\partial v}{\partial x}\right)\right].$$

3) The equation for a radial change in momentum:

$$\frac{\partial \rho u v}{\partial x} + \frac{1}{r}\frac{\partial \rho v^2 r}{\partial r} = -\frac{\partial \rho}{\partial x} + \frac{\partial}{\partial x}\left[(\mu + \mu_t)\left(\frac{\partial v}{\partial x} + \frac{\partial u}{\partial r}\right)\right] +$$
$$+ \frac{1}{r}\frac{\partial}{\partial r}\left[(\mu + \mu_t) r\left(2\frac{\partial v}{\partial r} - \frac{2}{3}\left(\frac{\partial u}{\partial x} + \frac{1}{r}\frac{\partial v r}{\partial r}\right)\right)\right] - 2\left(\frac{(\mu + \mu_t) v}{r^2}\right) + \frac{\rho w^2}{r}.$$

4) The equation for a circular change in momentum:

$$\frac{\partial \rho u v}{\partial x} + \frac{1}{r}\frac{\partial \rho v w r}{\partial r} = \frac{\partial}{\partial x}\left[((\mu + \mu_t))\frac{\partial w}{\partial x}\right] +$$
$$+ \frac{1}{r^2}\frac{\partial}{\partial r}\left[(\mu + \mu_t) r^3 \frac{\partial}{\partial r}\left(\frac{w}{r}\right)\right] - \frac{\rho v w}{r}.$$

5) The energy change equation:

$$\frac{\partial \rho h u}{\partial x} + \frac{1}{r}\left(\frac{\partial \rho h w r}{\partial r}\right) = \frac{\partial}{\partial x}\left[(\lambda + \lambda_t)\frac{\partial T}{\partial x}\right] + \frac{1}{r^2}\frac{\partial}{\partial r}\left((\lambda + \lambda_t) r\frac{\partial T}{\partial r}\right) +$$
$$+ (\mu + \mu_t)\left\{2\left[\left(\frac{\partial v}{\partial r}\right)^2 + \left(\frac{v}{r}\right)^2 + \left(\frac{\partial u}{\partial x}\right)^2\right] + \left[r\frac{\partial}{\partial r}\left(\frac{w}{r}\right)\right]^2 + \left(\frac{\partial w}{\partial x}\right)^2 +\right.$$
$$\left. + \left(\frac{\partial u}{\partial r}\right)^2 - \frac{2}{3}\left[\frac{1}{r}\frac{\partial}{\partial r}(r v) + \frac{\partial u}{\partial x}\right]^2\right\}.$$

6) The equation for a change in the kinetic energy of turbulent pulsations:

$$\frac{\partial \rho u k}{\partial x} + \frac{1}{r}\frac{\partial \rho v k r}{\partial r} = \frac{\partial}{\partial x}\left[\left((\mu + \frac{\mu_t}{\sigma_k})\right)\frac{\partial k}{\partial x}\right] +$$
$$+ \frac{1}{r^2}\frac{\partial}{\partial r}\left[\left(\mu + \frac{\mu_t}{\sigma_k}\right) r\frac{\partial k}{\partial r}\right] + G_k + G_b + \rho\varepsilon - Y_m$$

7) The equation for a change in the dissipation rate of turbulent energy:

$$\frac{\partial \rho u \varepsilon}{\partial x}+\frac{1}{r}\frac{\partial \rho v \varepsilon r}{\partial r}=\frac{\partial}{\partial x}\left[\left((\mu+\frac{\mu_t}{\sigma_k})\right)\frac{\partial \varepsilon}{\partial x}\right]+$$

$$+\frac{1}{r}\frac{\partial}{\partial r}\left[\left(\mu+\frac{\mu_t}{\sigma_k}\right)\frac{\partial \varepsilon}{\partial r}\right]+\rho C_1 G_\varepsilon+\rho C_2\frac{\varepsilon^2}{k+\sqrt{\nu\varepsilon}}+C_{1\varepsilon}\frac{\varepsilon}{k}C_{3\varepsilon}C_b\,.$$

where

$$h=C_pT+\frac{\left(u^2+v^2\right)}{2},$$

$$C_1=\max\left[0.43\frac{\eta}{\eta+5}\right],\ \ \eta=S\frac{k}{\varepsilon},\ \ S=\sqrt{2S_{ij}S_{ij}},$$

$$S=\begin{pmatrix}\frac{\partial u}{\partial x} & \frac{1}{2}\left(\frac{\partial u}{\partial r}+\frac{\partial v}{\partial x}\right) & \frac{1}{2}\frac{\partial w}{\partial x}\\ \frac{1}{2}\left(\frac{\partial u}{\partial r}+\frac{\partial v}{\partial x}\right) & \frac{\partial v}{\partial r} & \frac{1}{2}r\frac{\partial}{\partial r}\left(\frac{w}{r}\right)\\ \frac{1}{2}\frac{\partial w}{\partial x} & \frac{1}{2}r\frac{\partial}{\partial r}\left(\frac{w}{r}\right) & \frac{v}{r}\end{pmatrix},$$

$$C_k=\mu_t\left\{2\left[\left(\frac{\partial u}{\partial r}\right)^2+\left(\frac{\partial v}{\partial r}\right)^2+\left(\frac{v}{r}\right)^2\right]+\right.$$

$$\left.+\left(\frac{\partial u}{\partial r}+\frac{\partial v}{\partial x}\right)^2+\left(\frac{\partial w}{\partial x}\right)^2+\left(r\frac{\partial w/r}{\partial r}\right)^2\right\},$$

$$\mu=\rho C_\mu\frac{k^2}{\varepsilon},$$

$$\lambda_t=\lambda+\frac{C_p\mu_t}{\mathrm{Pr}_t},$$

$$Y_m=2\rho\varepsilon M_t^2,$$

$$M_t=\sqrt{\frac{k}{a^2}}.$$

When developing a mathematical two-dimensional model, the following boundary conditions were set:

- At the entrance to the vortex tube, total pressure $P = Pin$, the direction of the gas flow through the cosines and intensity of the turbulent pulsations, as well as the hydraulic diameter of the energy separation chamber were set.
- The symmetry condition:

$$\frac{\partial \varphi}{\partial r}=0,\quad v=0,$$

where: $\varphi=(\rho, p, u, w, \varepsilon, k)$.

- The condition of adhesion of the vortex tube on the walls $\vec{V}=0$.
- At the outlet of the vortex tube, static pressure equal to atmospheric pressure and the radial pressure distribution is: $\frac{\partial P}{\partial r}=\frac{\rho w^2}{r}$.

The system of equations was solved by the finite volume method. To determine gas-dynamic flows and approximate convective flows in cells, the second-order accuracy scheme was used [18].

The algorithm was as follows. First, 100 steps were taken with the Courant number equal to 5, then the Courant number was increased to 10, and 100 steps were taken, after the Courant number was increased to 50 and the calculation was performed until a stationary solution was obtained.

The physical formulation of the problem of the energy separation process in a vortex tube was considered under the same assumptions.

The mathematical formulation includes the following well-known equations [19-22]:

1) The continuity equation for a jet flow:

$$\frac{\partial \rho}{\partial t}+div(\rho\vec{v})=0.$$

2) The gas flow equation:

$$\frac{\partial}{\partial t}\left(\rho\vec{v}\right)+\nabla\left(\rho\vec{v}\vec{v}\right)=\nabla p+\nabla\left(\bar{\bar{\tau}}\right).$$

3) The energy change equation:

$$\frac{\partial}{\partial t}(\rho E)+\nabla(V(\rho E+p))=\nabla\left(k_{eff}\Delta T+\overline{\overline{\tau_{eff}}}V\right),$$

where

$$E=h-\frac{p}{\rho}+\frac{V^2}{2},$$

$$h=c_pT,$$

$$k_{eff}=k+k_t.$$

4) Equations of turbulence models (in order to minimize the computational cost for closing the system, the equations of the semi-empirical two-parameter standard are used) (k-ε)):

$$\frac{\partial k}{\partial t}+\nabla(Vk)=\nabla\left(\left(\mu+\frac{\mu_t}{\sigma_k}\right)\nabla k\right)+P_k-\varepsilon,$$

$$\frac{\partial k}{\partial t}+\nabla(V\varepsilon)=\nabla\left(\left(\mu+\frac{\mu_t}{\sigma_\varepsilon}\right)\nabla\varepsilon\right)+C_1\frac{\varepsilon}{k}P_k-C_2\frac{\varepsilon^2}{k},$$

where

$$\mu_t=\rho C_\mu\frac{k^2}{\varepsilon},$$

k – kinetic energy of turbulent pulsations;

ε – turbulent energy dissipation;

P_k – turbulent energy generation, $P_k=\mu_t S^2$, $S=\sqrt{2S_{ij}S_{ij}}$, $S_{ij}=\frac{1}{2}\left(\frac{\partial V_i}{\partial x_j}+\frac{\partial Vj}{\partial x_i}\right)$;

σ_k, σ_ε,C_1 ,C_2,– empirical constant turbulence models.

5) The ideal gas state equation:

$$p=\rho RT,$$

where R – universal gas constant;

T – temperature, K.

The following indicators were used as initial (boundary) conditions:

- static overpressure P_{st} =1 MPa;
- thermodynamic temperature T=300 K;
- speed $U_x = U_y = U_z = 0$;
- kinetic energy of turbulent pulsations $k = k_0$;
- turbulent energy dissipation $\varepsilon = \varepsilon_0$.

At the outlet to the vortex apparatus, the following boundary conditions were adopted:

- flow inhibition pressure, flow inhibition temperature, turbulent energy dissipation rate, kinetic energy of turbulent pulsations;
- at the outlets of hot and cold flows, pressure is static.

On the wall, adhesion conditions for gas are set:

$$\frac{\partial k}{\partial n}=0;\ \varepsilon=\frac{c_\mu^{3/4}k_p^{1.5}}{ky_p}.$$

The system of equations was solved using the finite volume method. To determine the gas-dynamic flows and approximation of convective flows in the cells, the second-order accuracy scheme using the Rowe method was applied.

The problem was solved using the Ansus Fluent software package. This numerical simulation includes the following steps:

1. Construction of geometry of the region and the difference grid (in the Gambit preprocessor).
2. Setting thermophysical properties of gas.
3. Choosing a difference scheme.
4. Setting initial and boundary conditions.
5. Launching a task.
6. Analyzing results obtained

3 Results

By the method described above, studies were carried out and the results of numerical simulation of energy separation of the vortex flow in two-dimensional and three-dimensional approximations were obtained.

The studies were carried out at the following inlet nominal pressures – P_{nom} = 4, 5, and 7.5 MPa with different flow swirl angles.

Figure 3 shows that the effective separation of temperatures does not depend on total pressure at the inlet to the vortex tube. It depends on changes in the swirl angle.

With an increase in the swirl angle, the temperature difference between hot and cold flows increases. If the swirl angles are excessively large, the opposite effect is observed, temperature at the periphery of the vortex decreases, and in the center, temperature increases. The best effect of energy separation is observed at a twist angle tan (α) = 3.5.

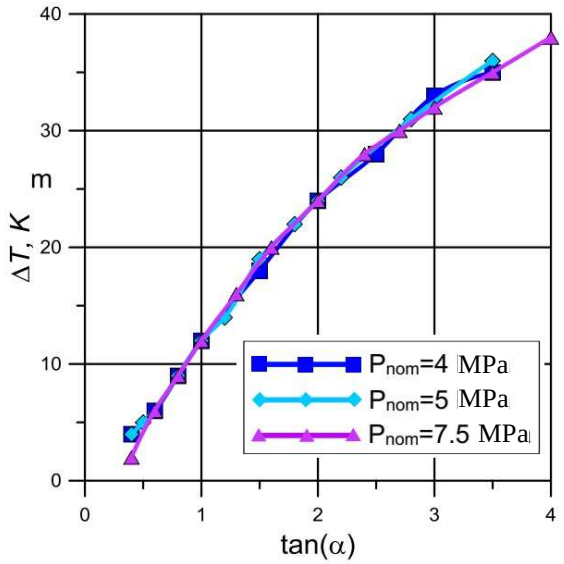

Fig. 3. The dependence of changes in temperature of hot and cold flows on the swirl angle

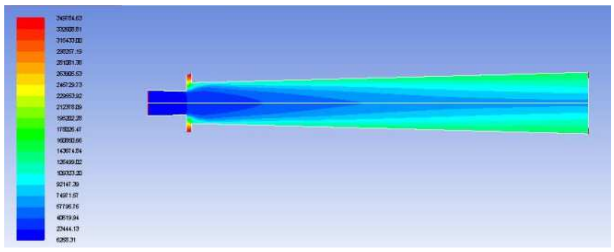

Fig. 4. Absolute Pressure Field

Figures 4 ... 6 show the fields of absolute pressure, total temperature, and Ma-ha number in a vortex tube with total pressure P = 4MPa and flow swirl angle tan (α) = 3.5.

Figure 4 shows that when the hot flow moves to the outlet, pressure increases uniformly, while at the outlet of the cooled flow, it decreases. At the periphery of the vortex, along the walls of the energy separation chamber, pressure increases and gradually decreases towards the center.

Figure 5 shows the distribution of the total temperature.

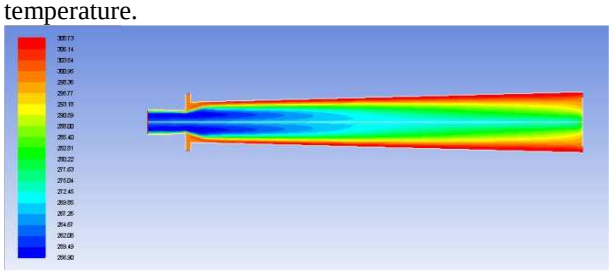

Fig. 5. Total temperature field

From the total temperature field (Figure 5), it can be observed that a temperature increase occurs in the near-wall region and reaches 308 K at the exit. At the same time, a noticeable decrease in temperature is observed in the central part. It is 285 K.

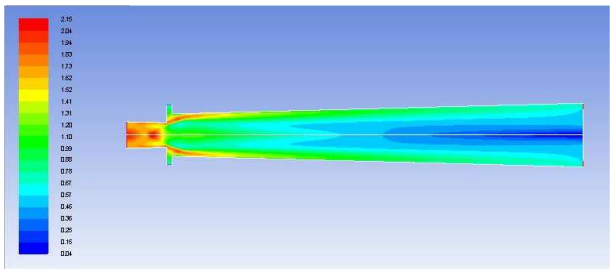

Fig. 6. Mach number field

Figure 6 shows that at the outlet of cooled gas, the Mach number is more than 1; consequently, cooled gas flows out at a supersonic speed, while the heated gas flows out at a supersonic speed.

To determine the effect of various turbulence models on the temperature separation of gas, the following results were obtained (Table 1).

Table 1 shows that when using different turbulence models, the fractions of cooled and hot flows changed insignificantly. The maximum temperature difference is shown by the turbulence model SST k – ω. Due to the simplicity of using the turbulence model and in order to simplify computational operations, we used the standard (k – ε) turbulence model [23].

Table 1. Results of calculations using various turbulence models

Turbulence model	Share of cold flow	Share of hot flow	flow temperature decrease, K	flow temperature increase, K
Realizable k–ε	0.35	0.65	20.82	9.93
Standard k– ε	0.37	0.63	22.83	12.87
RNG k–ε	0.31	0.69	18.52	8.58
Standard k–ω	0.35	0.65	23.69	10.41
SST k–ω	0.37	0.63	22.23	13.92
Spalart-Allmaras	0.39	0.61	23.79	11.1

To check the convergence of solutions, the grid was divided into 147840 cells and the temperature difference between the grids was 25.34 K. Having obtained a solution with a grid of 9240, the maximum temperature difference was 24.11, which is 1.23 degrees lower than the original one, the calculation error was 4.85 %. With a grid with 36960 cells, the difference was 0.56, the calculation error was 2 %, which confirms the accuracy of the solution.

For numerical modeling in the three-dimensional approximation, three computational regions were constructed. They differed by the cross-sectional area at the outlet of the hot flow of 1, 1.5 and 2 mm. Inlet nominal pressure was 7.5 MPa.

The figures below show the distribution of flow characteristics for the calculated region in a vortex tube.

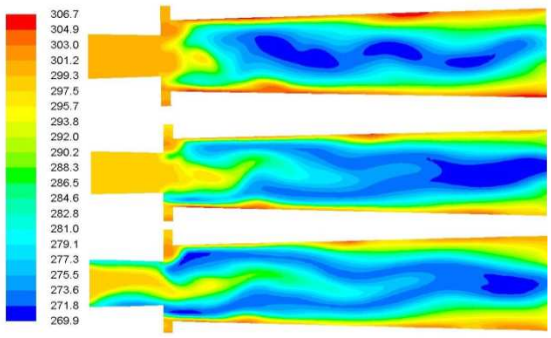

Fig. 7. Distribution field for total temperature

Fig. 7 shows an asymmetric flow pattern. With a gap of 2 mm, the temperature at the outlet of the cold flow remains constant

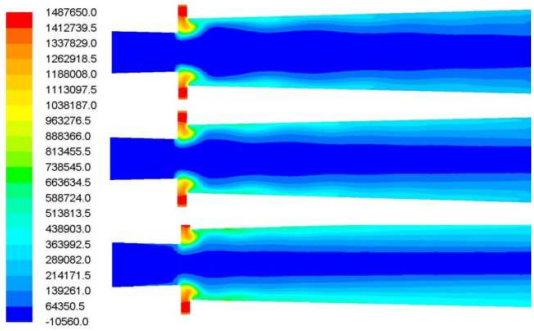

Fig. 8. Total pressure distribution field

Figure 8 shows that the gap size does not affect the distribution of total pressure.

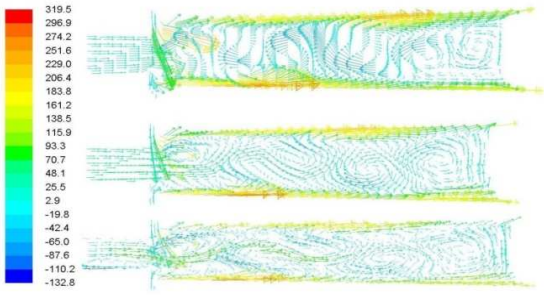

Fig. 9. The distribution field for the axial velocity component

Figure 9 shows a complex picture of the flow; it can be seen that the flow is unstable, turbulent. The figure shows the presence of large-scale vortices, which nucleate at the wall, and when swirling the flow [24, 25].

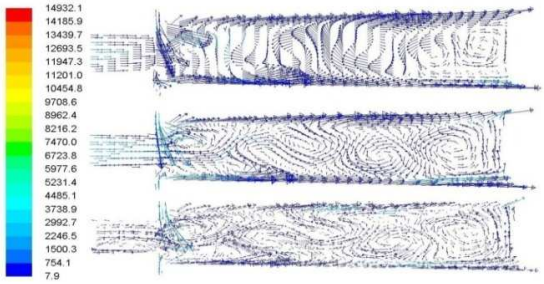

Fig. 10. Field of distribution of the ratio of turbulent viscosity to laminar viscosity for the computational domain

Figure 10 shows the presence of vortices formed due to the existence of two oppositely directed flows. The effect of turbulent viscosity affects the flow region near the wall. With a decrease in the exit gap, the two flows mix, forming large eddies in the swirl region [26].

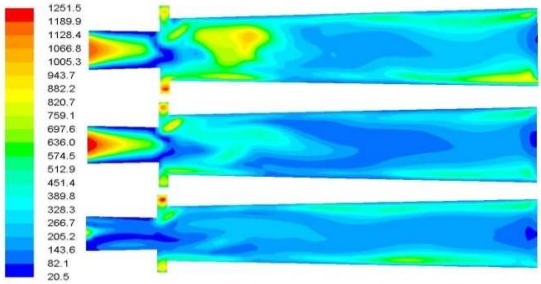

Fig. 11. Field of distribution of the ratio of turbulent viscosity to laminar viscosity for the computational domain

Figure 11 shows that with a gap of 1 mm, the viscous flow prevails at the beginning, when two flows are mixed, while as it approaches the exit of the hot flow, its effect decreases. With a gap of 2 mm, the opposite picture is observed; it is seen that the viscous sublayer zone prevails at the exit of the hot flow.

Figure 12 shows that with gaps of 1 and 1.5 mm at the outlet of the hot flow, with an increase in the mass flow rate at the inlet of the vortex tube, the temperature curve for the cooled flow decreases linearly, for the gap of 2 mm, the temperature is constant. With gaps of 1.5 and 2 mm, the temperature of gas at the outlet does not change, i.e., the size of the gap greatly affects the temperature separation.

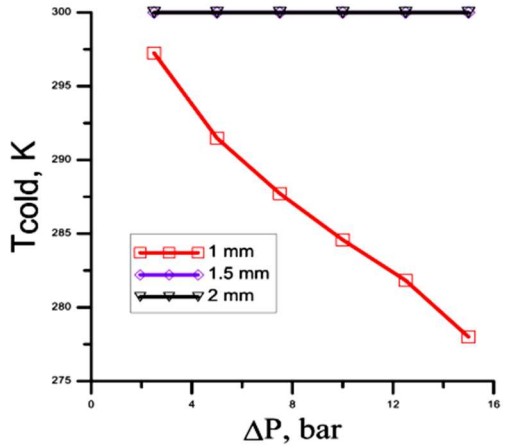

Fig. 12. The dependence of cooled gas temperature on the pressure drop

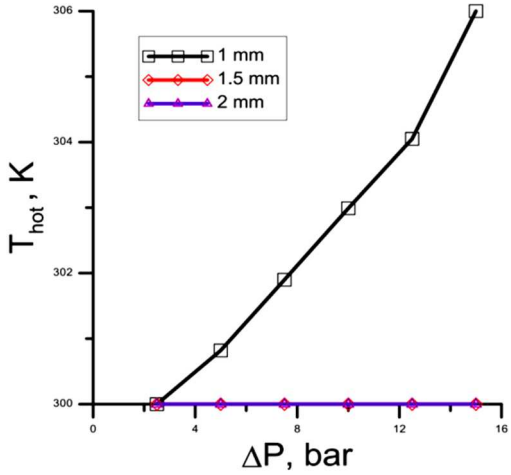

Fig. 13. The dependence of heated gas temperature on differential pressure

Figure 13 shows that maximum heating of the flow is observed with a gap of 1 mm at the outlet of the hot flow. With gaps of 1.5 and 2 mm, the gas temperature remains constant, the flow is not heated.

Figure 14 shows that the effect of mass flow is significant only for a vortex tube with a gap of 1 mm at the outlet of the hot flow. For geometries with large gaps of 1.5 mm and 2 mm, the effect of the mass flow rate on the cooling rate is not observed, the temperature at the outlet of cold gas remains constant.

Figure 15 shows that for a vortex tube with a gap of 1 mm, an increase in the mass flow rate affects flow heating intensity. With gaps of 1.5 or 2 mm, temperature at the outlet of the hot flow does not change. Table 2 shows fractions of the cooled and heated flows depending on the cross-sectional area at the outlet of the hot flow.

Table 2. The dependence of shares of cooled and heated flows on the cross-sectional area at the outlet of the hot flow

Value of the gap at the outlet of the hot flow, mm	Share of cooled flow, %	Share of heated flow, %
1	0.25016	0.75805
1.5	0.1152	0.8943
2	0.022	0.9986

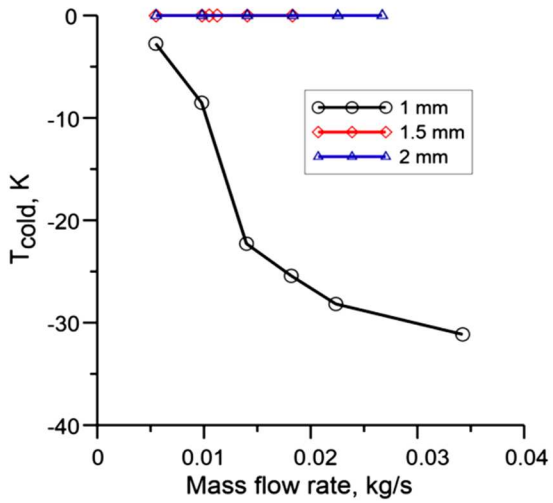

Fig. 14. The dependence of temperature at the outlet of the cold flow on the mass flow rate determined by differential pressure

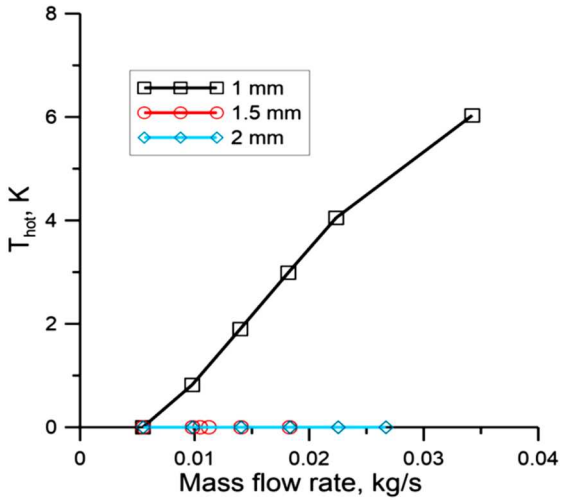

Fig. 15. The dependence of temperature at the outlet of the hot flow on the mass flow rate specified by differential pressure

Table 2 shows that with an increase in the gap at the outlet of the hot flow, the amount of intake air at the outlet of the cold stream increases. With a gap of 1 mm, this value was 0.00821 kg/s, with a gap of 1.5 mm, it was 0.0098 kg/s, with a gap of 2 mm – 0.0205 kg/s.

From the above dependency data, we can conclude that the size of the gap at the outlet of the hot flow affects the intensity of temperature separation. With large gaps at the outlet of the hot flow, the generated turbulence is large-scale, and since its concentration decreases, the efficiency of temperature separation decreases.

Due to the fact that with a decrease in the radius of the nozzle for the exit of the hot flow, the generation of turbulence increases unlimitedly, it is clear that with a decrease in the diameter of the vortex chamber, the efficiency of temperature separation increases. However, it is necessary to take into account the boundary conditions in viscous gas on a solid impermeable wall, as well as the existing turbulence at a certain distance from this wall [27].

4 Conclusion

The developed mathematical models and the results of interaction of vortices make it possible to reveal the nature of the vortex effect and calculate the values of convective flows at the oulet, as well as determine their distribution parameters in the energy separation chamber.

A two-dimensional flow in the Ranque-Hilsch vortex tube was simulated. Thermodynamic and hydrodynamic characteristics that confirm the effect of temperature separation were identified. The dependence of temperature separation on the swirl angle and inlet pressure was obtained. For a two-dimensional vortex tube model, calculations were performed using various turbulence models. It was found that the choice of a turbulence model for solving the equations does not affect the integral components of the fractions of cold and heated flows. It does not significantly affect the temperature separation in the vortex chamber.

A numerical simulation of the three-dimensional flow of a gas stream in a Rank-Hilsch vortex tube has been carried out. Thermodynamic and hydrodynamic characteristics are obtained that confirm the effect of temperature separation of the flow.

A study of the effect of the cross sectional area for hot gas on temperature separation was conducted. It was found that for a vortex tube with a smaller cross-sectional area at the outlet of the hot flow, the efficiency of temperature separation is much higher, while for a vortex tube with a larger cross-sectional area at the outlet of the hot flow, the temperature does not change.

Vortex devices remain a relevant research subject for many scientists. Knowledge about the processes occurring in vortex tubes will allow us to create a more accurate mathematical model that will increase the energy efficiency of plants and make it possible to assess new devices at the design stage and expand the scope of their applications in technological processes.

References

1. A.P. Merkulov, *Vortex effect and its application in engineering* (Mashinostroenie, Moscow, 1969) 183 p.
2. G.F. Nellis, S.A. Klein, *The application of vortex tubes to refrigeration cycles*, in: *9th Int. Refrigerat. and Air Condition. Conf.* (West Lafayette, USA, 2002)
3. B.L. Ivanov, B.G. Ziganshin, R.F. Sharafeev, I.R. Sagbiev, *Theory atomization fluid nozzles*, Bull. of Kazan State Agrar. Univer., **14(2(53))**, 95–99 (2019)
4. B.L. Ivanov, B.G. Ziganshin, A.I. Rudakov, M.A. Lushnov, *Assessment of distribution of drops of a disinfecting liquid by the surface processed*, Bull. of Kazan State Agrar. Univer., **14(3(54))**, 103–107 (2019)
5. R. Sabirov, A. Valiev, L. Karimova, A. Dmitriev, D. Khaliullin, *Influence of physical factors on viability of microorganisms for plant protection*, in: *18th Int. Sci. Conf. Engineer. for Rural Developm. Proc*., vol. 18 (Latvia Univer. of Life Sci. and Technol. Faculty of Engineer., Jelgava, 22–24 May 2019) pp. 555–562
6. S. Eiamsa-ard, P. Promvonge, *Review of Ranque-Hilsch effects in vortex tubes*, Renew. Sustain. Energy Rev., **12(7)**, 1822–1842 (2008)
7. A.I. Leont'ev, *Gasdynamic methods of temperature stratification*, Fluid dynamics, **37(4)**, 512–536 (2002)
8. C.D. Fulton, *Comments on the vortex tube*, J. ASRE Refrigerat. Engng., **58** (1950)
9. T. Cockerill, *Ranque – Hilsh vortex tube*, Master thesis (University of Cambridge, 1995)
10. A.S. Noskov, A.V. Chait, A.P. Butymova et al., *Energy effectiveness and economics expediency of using of climatic systems based on vortex tube*, Magaz. of civil engineer., **1**, 17–23 (2011)
11. S. Eiamsa-ard, P. Promvonge, *Review of Ranque-Hilsch effects in vortex tubes*, Renew. Sustain. Energy Rev., **12**, 1822–1842 (2008)
12. C.M. Gao, *Experimental study on the Ranque-Hilsch vortex tube*, PhD thesis (Techn. Univer., Eindhoven, 2005)
13. Y. Xue, *The working principle of a Ranque–Hilsch vortex tube*, PhD thesis (School of Mechan. Engineer.; Univer. of Adelaide, Australia, 2013)
14. Y. Xue, M. Arjomandi, R. Kelso, *Experimental study of the thermal separation in a vortex tube*, Exp. Therm. Fluid Sci., **46**, 175–182 (2013)
15. C. Gao, *Experimental study on the Ranque – Hilsh vortex tube*, PhD Study (2005) 151 p.
16. W. Fröhlingsdorf, H. Unger, *Numerical investigations of the compressible flow and the energy separation in the RanqueeHilsch vortex tube*, Int. J. of Heat and Mass Transfer, **42**, 415–422 (1999)
17. T. Farouk, B. Farouk, A. Gutsol, *Simulation of gas species and temperature separation in the counter-flow RanqueeHilsch vortex tube using the large eddy simulation technique*, Int. J. of Heat and Mass Transfer, **52**, 3320–3333 (2009)
18. U. Behera, P.J. Paul, S. Kasthurirengan, R. Karunanithi, S.N. Ram, K. Dinesh et al., *CFD analysis and experimental investigations towards optimizing the parameters of RanqueeHilsch vortex tube*, Int. J. of Heat and Mass Transfer, **48**, 1961–1973 (2005)
19. M. Attalla, H. Ahmed, M. Salem Ahmed, A. AboEl-Wafa, *Experimental investigation for thermal performance of series and parallel Ranque-Hilsch vortex tube systems*, Appl. Thermal Engineer., **123**, 327– 339 (2017)
20. M. Alizadeh, *Three dimensional numerical (3D CFD) study of effect of pressure-outlet and pressure-farfield boundary conditions on heat transfer predictions inside vortex tube*, Progr. in

Solar Energy and Engineer. Syst., **2(1**), 21–25 (2018)

21. T. Dutta, K.P. Sinhamahapatra, S.S. Bandyopadhyay, *Numerical investigation of gas species and energy separation in the Ranquee-Hilsch vortex tube using real gas model,* Int. J. Refrigerat., **34**, 2118–2128 (2011)
22. A.S. Noskov, V.N. Alekhin, A.V. Khait, *Numerical investigation of Ranque-Hilsch energy separation effect,* Appl. Mech. Mater., **281**, 355–358 (2013)
23. F.R. Menter, M. Kuntz, R. Langtry, *Ten Years of Experience with the SST Turbulence Model, In* K. Hanjalic, Y. Nagano, M. Tummers (eds.) *Turbulence, Heat and Mass Transfer 4* (Begell House Inc., 2003) pp. 625–632
24. S.V. Alekseenko, P.A. Kuibin, V.L. Okulov, *Theory of Concentrated Vortices: an Introduction* (Springer-Verlag, Berlin; Heidelberg, 2007)
25. S.S. Abdurakipov, V.M. Dulin, D.M. Markovich, *Self-oscillations in a jet flow and gaseous flame with strong swirl,* Thermophys., Aeromech., **25**, 379–386 (2018)
26. K. Oberleithner, M. Sieber, C.N. Nayeri et al., *Three–dimensional coherent structures in a swirling jet undergoing vortex breakdown: stability analysis and empirical mode construction,* J. Fluid Mech., **679**, 383–414 (2011)
27. R. Mullyadzhanov, S. Abdurakipov, K. Hanjalić, *Helical structures in the near field of a turbulent pipe jet,* Flow, Turbulence and Combust., **98(2)**, 367–388 (2017)